Herschel/PACS spectroscopy
of trace gases of the stratosphere of Titan[*]

M. Rengel[1], H. Sagawa[1],[**], P. Hartogh[1], E. Lellouch[2], H. Feuchtgruber[3], R. Moreno[2], C. Jarchow[1], R. Courtin[2],
J. Cernicharo[4], and L. M. Lara[5]

[1] Max-Planck-Institut für Sonnensystemforschung, Max-Planck-Str. 2, 37191 Katlenburg-Lindau, Germany
e-mail: rengel@mps.mpg.de
[2] LESIA – Observatoire de Paris, CNRS, Université Paris 6, Université Paris-Diderot, 5 place Jules Janssen, 92195 Meudon, France
[3] Max-Planck-Institut für extraterrestrische Physik, Giessenbachstrasse, 85748 Garching, Germany
[4] Departamento de Astrofísica, Centro de Astrobiología, CSIC-INTA, Torrejón de Ardoz, 28850 Madrid, Spain
[5] Instituto de Astrofísica de Andalucía (CSIC), 18008 Granada, Spain

ABSTRACT

Aims. We investigate the composition of Titan's stratosphere from new medium-resolution far-infrared observations performed with the full range of *Herschel*'s Photodetector Array Camera and Spectrometer (PACS) (51–220 μm at a resolution $\lambda/\Delta\lambda$ ranging from 950 to 5500 depending on wavelength and grating order).
Methods. Using PACS, we obtained the spectral emission of several features of the Titan's stratosphere. We used a line-by-line radiative transfer code and the least-squares fitting technique to infer the abundances of the trace constituents.
Results. Numerous spectral features attributable to CH_4, CO, HCN, and H_2O are present. From the flux density spectrum measured and by a detailed comparison with synthetic spectra, we constrain the stratospheric abundance of CH_4, which is assumed to be constant with altitude, to be 1.29 ± 0.03%. Similarly, we constrain the abundance of CO to be 50 ± 2 ppm, and the HCN vertical distribution consistent with an increase from 40 ppb at ∼100 km to ∼4 ppm at ∼200 km, which is an altitude region where the HCN signatures are sensitive. Measurements of three H_2O rotational lines confirm the H_2O distribution profile recently obtained with *Herschel*. Furthermore, we determine the isotopic ratios $^{12}C/^{13}C$ in CO and HCN to be 124 ± 58, and 66 ± 35, respectively. Comparisons between our results and the values derived with other instruments show that our results are consistent with the vertical distributions and isotopic ratios in previous studies, except for the HCN distribution obtained with *Cassini*/CIRS, which does not agree with the PACS lines at the 1-σ confidence interval.

Key words. planets and satellites: atmospheres – planets and satellites: individual: Titan – techniques: spectroscopic

1. Introduction

The nitrogen (N_2)-dominated atmosphere of Titan, Saturn's largest moon, exhibits a great diversity and complexity of molecules and high organic material abundances. Many species are formed in the upper atmosphere (above 600 km) by interaction of solar UV photons, energetic ions/electrons, and cosmic-ray particles, which initiate a complicated photochemical network. For several of these molecules, the region between the upper atmosphere and their condensation sink (60–100 km) is a transition region. In the stratosphere (40–320 km), complex chemistry is still in action, and this region is probed mainly with thermal infrared measurements. Previous studies of Titan's submillimetre and infrared spectra from space (e.g. the Infrared Space Observatory (ISO) and *Cassini*/Composite InfraRed Spectrometer (CIRS)) and ground-based facilities at different spectral resolutions have revealed many specific aspects of the molecular composition, permitted a detailed investigation of the photochemical and dynamical processes in Titan's

atmosphere, and confirmed the seasonal behaviour of Titan's atmospheric composition (e.g. Roe et al. 2004; de Kok et al. 2007; Coustenis et al. 2007; Teanby et al. 2009a, 2012; Rengel et al. 2011). New observations at different spectral ranges, higher spectral resolution and sensitivity, and at different temporal coverage during a Titan's year (29.5 Earth years) offer the opportunity of exploring and helping to advance the study of the abundance distribution (e.g. new abundance constraints and rate of seasonal variations).

The advent of the *Herschel* Space Observatory (Pilbratt et al. 2010) allowed to determine the stratosphere abundances of CH_4, CO and HCN with the Spectral and Photometric Imaging Receiver (SPIRE) covering the 194–671 μm spectral region with an spectral resolution of 0.04 cm^{-1} (Courtin et al. 2011), to detect HNC with the Heterodyne Instrument for the Far-Infrared (HIFI; Moreno et al. 2011), and infer the vertical profile of H_2O over the 100–450 km altitude range by combining data from HIFI and the Photodetector Array Camera and Spectrometer (PACS; Moreno et al. 2012).

In this paper, we report the results from a full grating resolution spectra of Titan at 51–220 μm (5878–1363 GHz) taken with PACS (Poglitsch et al. 2010) onboard *Herschel*. Although it covers a smaller spectral range than *Cassini*/CIRS and a range similar to that of ISO/LSW ([17–1000] and [2.4–196] μm,

---

Table 1. Summary of the observations.

Obs. ID	Start time [UTC]	T_{obs} [s]	Range^a [μm]
1342199145	23 June 2010 00:42:40	1140	51–073^{B2A}, 102–146^{R1}
1342199146	23 June 2010 01:03:48	2268	70–105^{B2B}, 140–220^{R1}
1342211198	15 Dec. 2010 05:56:53	4051	55–072^{B3A}, 165–216^{R1}
1342211199	15 Dec. 2010 07:06:33	3509	70–099^{B2B}, 140–198^{R1}
1342211200	15 Dec. 2010 08:07:14	1983	51–071^{B2A}, 102–141^{R1}

Notes. [a] Spectral band.

respectively), PACS has a higher spectral resolution than previous instruments (ISO/SWS and LSW have resolving powers of 1000–2500 and 200, respectively, and *Cassini*/CIRS has a spectral resolution of 0.5 cm^{-1}). We report the gases identified in the spectra, derive their abundances, and compare them with previous studies. A few isotopic lines are identified, from which we estimate the isotopic ratios ^{12}C/^{13}C in CO and HCN. More possible detections of isotopes are limited by the sensitivity of the PACS observations and the weakness of the lines, which can easily be confused with noise.

2. Observations and data reduction

In the framework of the program "Water and Related Chemistry in the Solar System", (Hartogh et al. 2009), full-range observations of Titan were performed on June 23 and December 15, 2010 (Table 1). Observations were carried out in chopped-nodded PACS range spectroscopy modes (Poglitsch et al. 2010), at Nyquist/spectral energy distribution (SED; second and first orders of the grating spectrometer) and at high spectral sampling density (third and first orders) for the June and December observations, respectively.

The entire spectral range of PACS was measured at full instrumental resolution $\lambda/\Delta\lambda$, ranging from 950 to 5500 depending on wavelength and grating order (Poglitsch et al. 2010). Since blue and red spectrometer data are acquired in parallel, several spectral ranges were observed in overlap. To minimise spectral contributions from Saturn, Titan was observed at the largest feasible elongations from Saturn (168″ and 173″ on 23 June and 15 December 2010, respectively). The data processing from Level 0 to 1 was carried out by standard PACS pipeline modules using the *Herschel* interactive processing environment (HIPE v.4 and v.6). All subsequent processing (flat-fielding, outlier removal and rebinning) was carried out with standard interactive data language (IDL) tools. Because the absolute calibration accuracy is limited by detector response drifts and slight pointing offsets[1], the resulting spectrum was divided by its continuum, a step that is not subject to changes through later HIPE releases. For spectral ranges covered more than once, the observation with the highest resolution was selected. When observations are covered with the same spectral band, an averaged observation was used to increase the signal-to-noise-ratio (S/N). The data adquired during different operational days were carefully compared to verify that no remarkable temporal changes in the instrumental characters and in seasonal changes in the atmosphere of Titan ocurred. Within the noise level, no variations were seen.

---

[1] http://herschel.esac.esa.int/

The composite spectrum is shown in Fig. 1. It shows several emission molecular signatures attributable to CH$_4$, CO, HCN, and H$_2$O, molecules that have been previously detected on Titan, but most line transitions are detected for the first time. We detected some faint emission features attributable to isotopologues above the noise (3–5% above the line-to-continuum ratio), the ^{13}CO (15–14) and (16–15), and the H^{13}CN (19–18) and (20–19) spectral lines.

3. Modelling the Titan PACS spectra and comparing them with the observed spectra

Our simulation package was developed based on the general forward and inversion model called microwave observation line estimation and retrieval (MOLIERE (v5); Urban et al. 2004; Rengel et al. 2010; Sagawa et al. 2010). The forward model consists of a line-by-line radiative transfer model that takes into consideration a homogeneous spherically symmetric atmosphere of Titan (altitudes from 0 to 800 km) and instrumental functions (where the *Herschel* beam profile and the PACS spectral response are considered, we assumed a uniform brightness temperature on the disk and Titan as a point-source). CH$_4$, CO, HCN, and H$_2$O (and their isotopologues) were considered for the line opacity calculation. Isotopic ratios were initially set by adopting the values derived by Courtin et al. (2011), when available, and terrestrial ratio ones. For the thermal profile of Titan's atmosphere, we adopted the distribution used in Moreno et al. (2011), a combination of the *Huygens* Atmospheric Structure Instrument (HASI) profile (Fulchignoni et al. 2005) below 140 km, and *Cassini*/CIRS stratospheric temperatures (Vinatier et al. 2010) above 140 km.

The a priori molecular mixing ratios adopted in this study are those derived by Niemann et al. (2010) and de Kok et al. (2007) for CH$_4$ and CO, respectively, and the a priori profile is that derived by Marten et al. (2002) for HCN. Spectroscopic parameters such as the transition frequency and the line intensity were derived from the HITRAN 2008 compilation (Rothman et al. 2009), and line strengths for CH$_4$ were taken from Boudon et al. (2010). As previously mentioned, we analysed the PACS spectra on the basis of the line-to-continuum ratios. We used the collision-induced absorption (CIA) coefficients of N$_2$ and CH$_4$ based on the formulation of Borysow & Frommhold (1986), Borysow & Frommhold (1987), and Borysow & Tang (1993). A comparison between our forward model and that reported in Moreno et al. (2012) under the condition of a pencil beam (a one-dimensional beam, i.e., the beam width is zero) in the nadir viewing geometry shows that they agree well within 3%. The PACS spectral response modelling ($\lambda/\Delta\lambda \sim 1000$–5000, which depends on the wavelength and grating diffraction conditions) was performed by following the descriptions by Poglitsch et al. (2010), and the related documents on the *Herschel* Science Center[1]. A comparison between observed data and synthetic spectra is shown in Fig. 1.

The best-fit between the observed and modelled spectra was performed simultaneously by least-squares fitting, that is, minimising χ^2. As sources of uncertainties we considered measurement and modelling errors. While the first one was considered as the standard deviation of several ObsIds (when available) and the oscillations about the smooth spectral continuum, modelling errors were considered as the variance caused by the residual between the measured and fitted fluxes, set it with a value of 3% and 1% for the blue and red bands, respectively. We
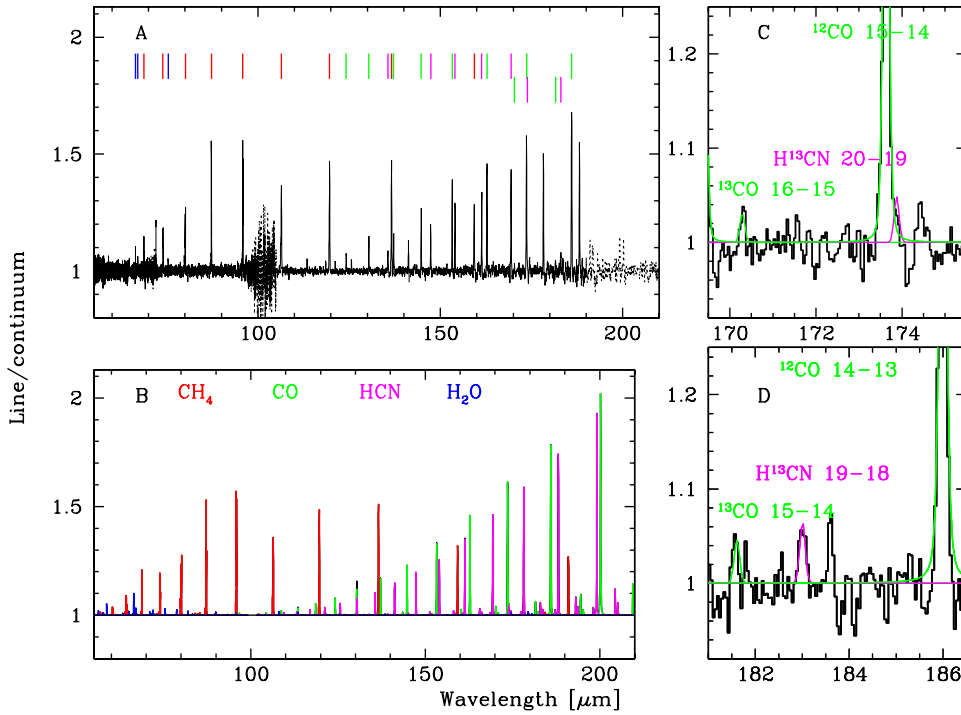
Fig. 1. A) black line shows the PACS spectrum of Titan, expressed in line-to-continuum ratios. The coloured marks at the top show the selected lines and transitions for the analysis in Sect. 4. The dashed line indicates spectral regions affected by spectral leakage due to grating order overlap. **B)** best-fit synthetic spectra indicating the signatures attributable to CH_4, CO, H_2O, and HCN (Sect. 4). **C)–D)** the [170–176] and [181–187] μm regions of the PACS spectrum displaying signatures of the isotopologues, along with the best-fit model with the detected isotopic variants.

quote our results at 1-σ significance level, which is given by a change $\Delta\chi^2 = \chi^2 - \chi^2_{\min}$ of 1.

4. Mixing ratios of individual trace constituents

CH_4: CH_4 is the second-most abundant gas in Titan's atmosphere, and its origin is unknown. Possible scenarios range from a continuous resupply to the atmosphere from a reservoir (from Titan's interior) to a recent and transitory component of the atmosphere (Nixon et al. 2012). The CH_4 distribution has been determined previously, it is uniformly mixed in the entire stratosphere (Niemann et al. 2005), and abundances of 1.6 ± 0.5%, 1.48 ± 0.09% between 76 and 140 km, and 1.33 ± 0.07% were measured previously (Flasar et al. 2005; Niemann et al. 2010; Courtin et al. 2011), respectively. We used selected CH_4 lines, simulated the observed spectra using the forward model (adopting several constant abundance distributions), and determined the best-fit (Figs. 2, 3). We found a best-fit volume-mixing ratio of 1.29 ± 0.03%, which is consistent with the SPIRE determination.

CO: CO is the fourth-most abundant molecule in Titan's atmosphere. It is not established whether the CO in Titan's atmosphere is primordial (from the interior or surface, Wilson & Atreya 2004) or due solely to external sources. As first shown by Hörst et al. (2008), the influx of O^+ from Saturn's magnetosphere into Titan (Hartle et al. 2006) can lead to the formation of CO through reactions between ground-state $O(^3P)$ and CH_3. Recent observations suggest that CO in Titan is uniformly mixed throughout Titan's atmosphere (Gurwell 2004; Baines et al. 2006; de Kok et al. 2007). Such a profile can be expected if its long chemical lifetime in the oxygen-poor Titan atmosphere is considered (~10^9 years, Yung et al. 1984). In this study, we retrieved the CO abundance by assuming a vertically
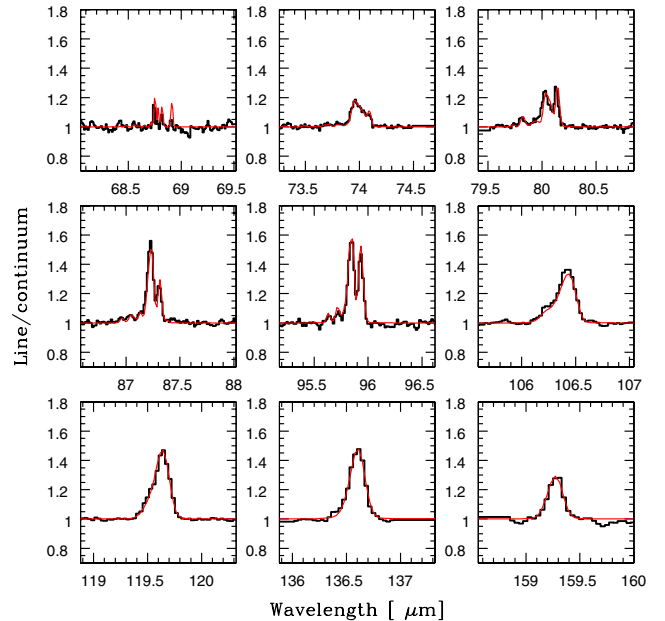

Fig. 2. Observed and best-fit simulated CH_4 lines (black and red, respectively).

constant profile and simultaneously computed synthetic selected CO lines for several abundances. We found a best-fit volume-mixing ratio of 50 ± 2 ppm (Fig. 4), consistent with the results from *Herschel*/SPIRE of 40 ± 5 ppm (Courtin et al. 2011), *Cassini*/CIRS (de Kok et al. 2007) of 47 ± 8 ppm, the Atacama Pathfinder EXperiment (APEX)/ Swedish Heterodyne Facility Instrument (SHeFI) of 30^{+15}_{-8} ppm (Rengel et al. 2011), and the Submillimeter Array (SMA) of 51 ± 4 ppm (Gurwell et al. 2012). The PACS CO lines reported here are sensitive to
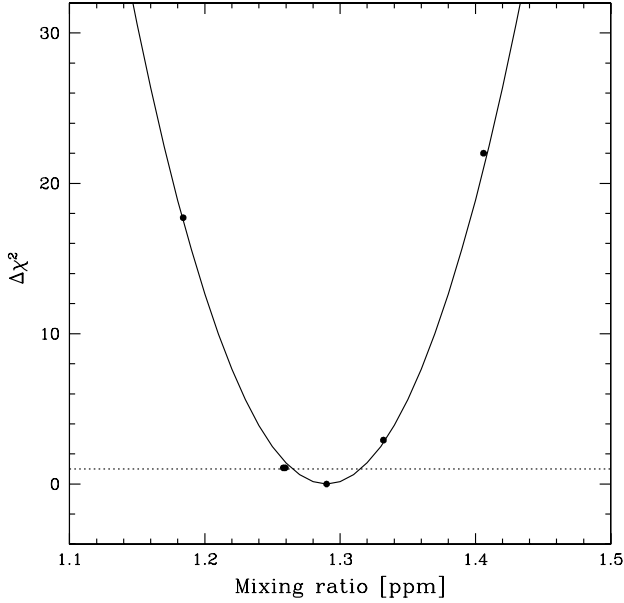
Fig. 3. Best-fit volume-mixing ratio and the 1-σ confidence limits.
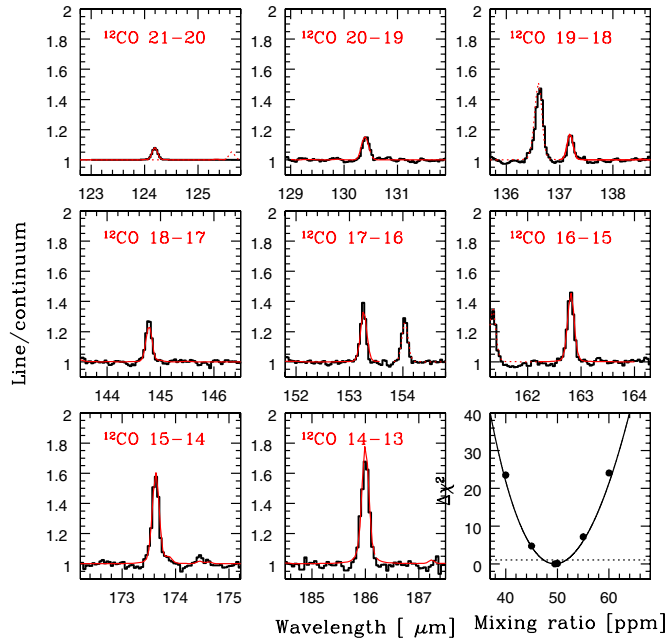

Fig. 4. Observed and best-fit simulated CO lines (black and red, respectively). The dashed lines show the best-fitting simulated lines of other species. Note that the observed CO line at 130.37 μm is overlapped by the HCN line at 130.24 μm. *Bottom-right panel*: best-fit volume-mixing ratio and the 1-σ confidence limits.

the [60–170] km range altitude.

HCN: HCN is generated photochemically in Titan's atmosphere from reactions of hydrocarbon radicals with atomic nitrogen. The latter is produced from EUV or electron impact on N_2, or possibly liberated as a result of cometary impacts (Sekine et al. 2011). HCN is produced above 300 km (Lara et al. 1996; Wilson & Atreya 2004) and removed by condensation deeper in the atmosphere. This sets up a concentration gradient. A more recent alternative suggests that HCN is thermodynamically generated via a shock chemistry under lightning discharges in the low atmosphere (Kovács & Turányi 2010). We analysed the
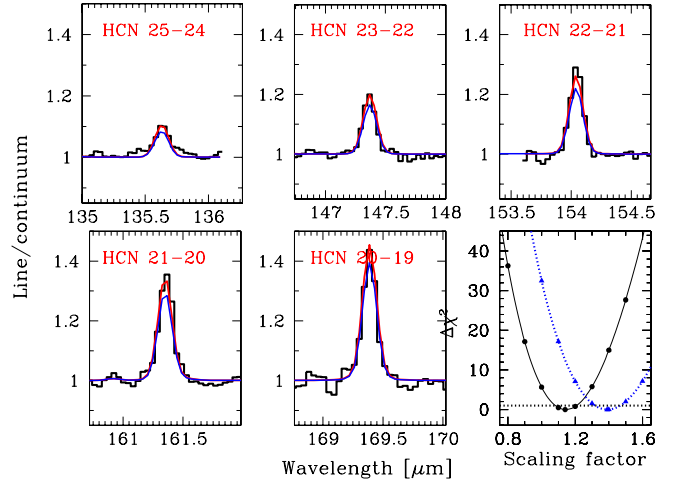
Fig. 5. Observed and best-fit simulated HCN lines (black and red, respectively). Blue spectra indicate the simulated spectra using the abundance profile derived from Vinatier et al. (2007).

observed spectra by scaling a well-probed reference distribution with a vertically constant factor. This offers a reliable result under the current data quality and has also been successfully applied for the *Herschel*/SPIRE observations (Courtin et al. 2011), which also facilitates the inter-comparisons. We retrieved the scaling factor applied to the adopted distribution of Marten et al. (2002), minimising χ^2, and using a simultaneous combination of five HCN lines (selected as good-quality lines in terms of the baseline corrections). We obtained a scaling factor of 1.14 ± 0.06 as a best-fit to the observed spectrum (Fig. 5), consistent with the value of 1.02 ± 0.13 derived with SPIRE (Courtin et al. 2011). For comparisons the simulated lines following the distribution obtained by *Cassini*/CIRS (Vinatier et al. 2007) are also shown. The CIRS distribution disagrees with the PACS observations at the 1-σ level. We discarded the difference in geometry as the source of the inconsistency because a disk-averaged spectrum gives preferential weight to low latitudes. Although CIRS data at southern latitudes show no variation during 3.5 years (Teanby et al. 2009b), temporal variability as the source of discrepancy is not completely ruled out: some scatter in the HCN values in Teanby et al. (2009b) is compatible with the differences we notice, and the PACS and CIRS data were not recorded in the same period. The absolute abundance in the CIRS data seems to be a possible source because by multiplying the Vinatier et al. (2007) distribution by factor of 1.39 a good fit is recovered. The analysis presented here confirms the results from Marten et al. (2002). Figure 6 shows our retrieved HCN vertical distribution (sensitive to an altitude between 100 and 200 km) compared with the distributions obtained with *Cassini*/CIRS and *Herschel*/SPIRE.

H_2O: the origin of Titan's water remains puzzling. Based on HIFI observations of the H_2O Enceladus torus, Hartogh et al. (2011) found that Enceladus is a source for Titan water, but not sufficient given the early estimates of the influx OH/H_2O fluxes into Titan as summarized by Strobel (2010). By using combined PACS and HIFI observations of water lines in Titan, covering several periods in 2010 and 2011 and with a higher S/N, Moreno et al. (2012) determined the H_2O profile, and their estimates of the OH/H_2O now offer a possible reconciliation with the input flux into Titan caused by the plume activity of
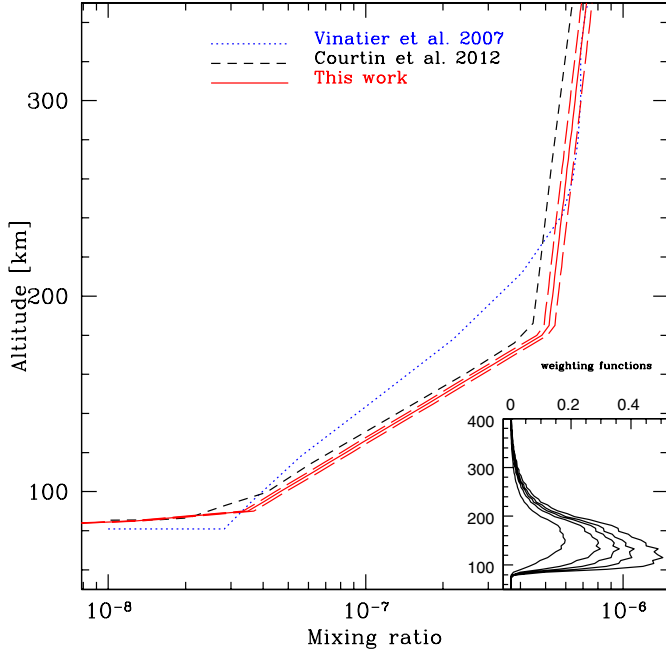
Fig. 6. Distribution of HCN (solid line) compared with the profile obtained by Vinatier et al. (2007) from *Cassini*/CIRS data at 15°S latitude (dotted line) and by Courtin et al. (2011) from *Herschel*/SPIRE data (short dashes). Long-dashed lines show the 1-σ limit. The curves in the small box represent the weighting functions for each line. We used the same line order as in Fig. 5 (from left to right).

Enceladus. Measurements of water vapor in Titan's stratosphere have also been recently reported using *Cassini*/CIRS (Cottini et al. 2012). Both *Cassini* and *Herschel* observations indicate that the previous models over-predict the water abundance in Titan's lower stratosphere, but the two vertical abundance differ. The photochemical model developed by Krasnopolsky (2012) yields a H_2O profile that includes the O^+ flux. This profile lies between the *Herschel* (Moreno et al. 2012) and *Cassini* (Cottini et al. 2012) observations. We measured the transitions H_2O ($3_{30}-2_{21}$), H_2O ($3_{31}-2_{20}$), and H_2O ($3_{21}-2_{12}$) at 66.6, 67.1 and 75.4 μm, respectively. The H_2O ($3_{31}-2_{20}$) one is measured for first time. We simulated the spectra considering the semi-empirical S_a profile determined in Moreno et al. (2012). Figure 7 shows a comparison between the observed and modelled H_2O lines. S_a fits the line at 66.4 μm, but underestimates the lines at 67.1 and 75.4 μm by a factor of ~0.67. Considering the S/N limitations, we focused on the 66.4 μm line, and the S_a distribution is compatible with these PACS lines. Additional sources of discrepancies are the intensity variations within 10%, the differences of the radiative description among the forward models, and errors due to the incomplete radiative description.

Isotopic ratios: $^{13}C/^{12}C$ in CO and HCN: the detection of the isotopes ^{13}CO (15–14) and (16–15), and $H^{13}CN$ (19–18) and (20–19) is only marginal (Fig. 1). Their abundances are found by a least-squares fit, with errors at the 1-σ significance level. The derived isotopic ratio estimates are $^{12}C/^{13}C$ of 124 ± 58, and 66 ± 35 in CO and HCN, respectively. They are consistent with the terrestrial value of 89.3 given the error bars. The $^{12}C/^{13}C$ from this work is consistent with the measurements by SPIRE, CIRS, and SMA (Courtin et al. 2011; Vinatier et al. 2007; Gurwell 2004, 2008).
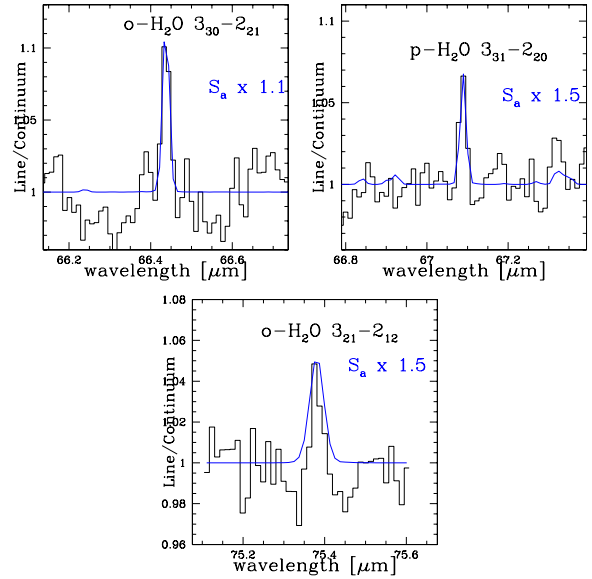

Fig. 7. Comparisons between synthetic spectra computed with the semi-empirical (S_a) profile of water (Moreno et al. 2012) and an ensemble of three PACS lines at 66.44, 67.09 (ObsId 1342211198) and 75.38 μm (ObsId 1342211199).

5. Conclusions

We reported the first observations obtained with the full range of *Herschel*/PACS of Titan. PACS produces a new survey of Titan's spectrum between 51 and 220 μm. Signatures attributable to CH_4, CO, HCN, and H_2O are detected.

We investigated the CH_4, CO, and HCN composition of Titan's stratosphere as seen by *Herschel*/PACS. Nine lines of CH_4 dominate the PACS spectrum and are consistent with an abundance of 1.29 ± 0.03%, which is consistent with the value obtained by SPIRE and that obtained in situ by the *Huygens*/Gas Chromatograph Mass Spectrometer (GCMS). Eight rotational lines of CO that dominate the PACS spectrum were selected to determine its abundance. Assuming it is well mixed, its abundance was found to be 50 ± 2 ppm, consistent with previous studies. Five lines of HCN were selected to retrieve the HCN vertical distribution. Our HCN mixing-ratio estimations, with a 1.14 scaling factor of the Marten et al. (2002) distribution between 100 and 200 km, are consistent with those with *Herschel*/SPIRE. The HCN distribution obtained by CIRS does not seem to reproduce the HCN lines observed with PACS well. Within the known sources of errors, the H_2O distribution proposed from previous *Herschel* observations produces a satisfactory fit to three H_2O lines detected. The ^{13}C isotope was detected in CO and HCN. We determined $^{12}C/^{13}C$ in CO and HCN on Titan (Sect. 4).

Limb observations of Titan's submillimetre radiation (e.g. in the 300–360, 540–660, and 1080–1280 GHz spectral ranges) are required to detect more rotational lines, measure rotational lines of isotopes, and winds in regions higher than the 200–1200 km altitude (Lellouch et al. 2010).

References

Baines, K. H., Drossart, P., Lopez-Valverde, M. A., et al. 2006, Planet. Space Sci., 54, 1552
Borysow, A., & Frommhold, L. 1986, ApJ, 311, 1043
Borysow, A., & Frommhold, L. 1987, ApJ, 318, 940
Borysow, A., & Tang, C. 1993, Icarus, 105, 175
Boudon, V., Pirali, O., Roy, P., et al. 2010, J. Quant. Spec. Radiat. Transf., 111, 1117
Cottini, V., Nixon, C. A., Jennings, D. E., et al. 2012, Icarus, 220, 855
Courtin, R., Swinyard, B. M., Moreno, R., et al. 2011, A&A, 536, L2
Coustenis, A., Achterberg, R. K., Conrath, B. J., et al. 2007, Icarus, 189, 35
de Kok, R., Irwin, P. G. J., Teanby, N. A., et al. 2007, Icarus, 191, 223
Flasar, F. M., Achterberg, R. K., Conrath, B. J., et al. 2005, Science, 308, 975
Fulchignoni, M., Ferri, F., Angrilli, F., et al. 2005, Nature, 438, 785
Gurwell, M. A. 2004, ApJ, 616, L7
Gurwell, M. A. 2008, in AAS/Division for Planetary Sciences Meeting Abstracts, BAAS, 40, 423
Gurwell, M. A., Butler, B. J., & Moullet, A. 2012, in AAS/Division for Planetary Sciences Meeting Abstracts, #312.12, 44
Hartle, R. E., Sittler, E. C., Neubauer, F. M., et al. 2006, Planet. Space Sci., 54, 1211
Hartogh, P., Lellouch, E., Crovisier, J., et al. 2009, Planet. Space Sci., 57, 1596
Hartogh, P., Lellouch, E., Moreno, R., et al. 2011, A&A, 532, L2
Hörst, S. M., Vuitton, V., & Yelle, R. V. 2008, J. Geophys. Res.: Planets, 113
Kovács, T., & Turányi, T. 2010, Icarus, 207, 938
Krasnopolsky, V. A. 2012, Planet. Space Sci., 73, 318
Lara, L. M., Lellouch, E., López-Moreno, J. J., & Rodrigo, R. 1996, J. Geophys. Res., 101, 23261
Lellouch, E., Vinatier, S., Moreno, R., et al. 2010, Planet. Space Sci., 58, 1724
Marten, A., Hidayat, T., Biraud, Y., & Moreno, R. 2002, Icarus, 158, 532
Moreno, R., Lellouch, E., Lara, L. M., et al. 2011, A&A, 536, L12
Moreno, R., Lellouch, E., Lara, L. M., et al. 2012, Icarus, 221, 753
Niemann, H. B., Atreya, S. K., Bauer, S. J., et al. 2005, Nature, 438, 779
Niemann, H. B., Atreya, S. K., Demick, J. E., et al. 2010, J. Geophys. Res. Planets, 115, 12006
Nixon, C. A., Temelso, B., Vinatier, S., et al. 2012, ApJ, 749, 159
Pilbratt, G. L., Riedinger, J. R., Passvogel, T., et al. 2010, A&A, 518, L1
Poglitsch, A., Waelkens, C., Geis, N., et al. 2010, A&A, 518, L2
Rengel, M., Sagawa, H., & Hartogh, P. 2010, Adv. Geosci., 19, 335
Rengel, M., Sagawa, H., & Hartogh, P. 2011, Adv. Geosci., 25, 173
Roe, H. G., de Pater, I., & McKay, C. P. 2004, Icarus, 169, 440
Rothman, L., Gordon, I., Barbe, A., et al. 2009, J. Quant. Spectros. Radiat. Transf., 110, 533
Sagawa, H., Hartogh, P., Rengel, M., de Lange, A., & Cavalié, T. 2010, Planet. Space Sci., 58, 1692
Sekine, Y., Genda, H., Sugita, S., Kadono, T., & Matsui, T. 2011, Nature Geosci., 4, 359
Strobel, D. F. 2010, Icarus, 208, 878
Teanby, N. A., Irwin, P. G. J., de Kok, R., et al. 2009a, Icarus, 202, 620
Teanby, N. A., Irwin, P. G. J., de Kok, R., & Nixon, C. A. 2009b, Roy. Soc. London Philos. Trans. Ser. A, 367, 697
Teanby, N. A., Irwin, P. G. J., Nixon, C. A., et al. 2012, Nature, 491, 732
Urban, J., Baron, P., Lauti, N., et al. 2004, J. Quant. Spectros. Radiat. Transf., 83, 529
Vinatier, S., Bézard, B., Fouchet, T., et al. 2007, Icarus, 188, 120
Vinatier, S., Bézard, B., Nixon, C. A., et al. 2010, Icarus, 205, 559
Wilson, E. H., & Atreya, S. K. 2004, J. Geophys. Res. Planets, 109, 6002
Yung, Y. L., Allen, M., & Pinto, J. P. 1984, ApJS, 55, 465